

## Spatial variations of stress drop within individual sequences: implications for earthquake triggering

\*xiaowei chen<sup>1</sup>, Rachel Abercrombie<sup>2</sup>, Colin Pennington<sup>1</sup>

1. University of Oklahoma Norman Campus, 2. Boston University

Stress drop is an important parameter not only related to fundamentals in earthquake source physics, but also high frequency ground motions. The rapidly increased seismicity in central US poses significant challenges to earthquake hazard modeling. In this study, we carefully analyze several individual clusters in Oklahoma. For each cluster, we perform a sensitivity test to obtain the parameter ranges that provide most stable results using a stacking EGF approach. Then, we test two hypotheses to assess if there is any robust scaling relationship that extends from small to large magnitude, and the stability of spatial variability. Our results suggest that the large earthquakes consistently have higher stress drop, however, there is not a general scaling relationship. The higher stress drop tends to be related to structural heterogeneity, and the spatial variability of stress drop is stable regardless of large earthquakes. These observations suggest that robust mapping of stress drop distributions would be important for future hazard assessment. To further understand the characteristics of large earthquakes, we perform detailed individual EGF to obtain independent estimates of stress drop. This analysis also enables us to investigate the complexity, rupture directivity and rupture velocity of the best-recorded earthquakes. The results suggest that M3-4 events involve significant complexity, including multiple sub-events and strong directivity effects.

Keywords: Stress drop, induced seismicity, spatial variations

## Toward the accurate stress drop estimation: improve corner frequency estimation with residual evaluation

\*Nana Yoshimitsu<sup>1</sup>, William Ellsworth<sup>1</sup>, Gregory Beroza<sup>1</sup>

1. Stanford University

In the last several years, disposal of wastewater increases the seismic activity in central United States, especially in Oklahoma. The similarity or difference of the source characteristics between induced and natural earthquakes would contribute to hazard assessment. While stress drop is one of the most important source parameter, its difficulty of accurate estimation is well known. The common process in the stress drop estimation need to obtain the corner frequency by comparing the spectral ratio of the co-located event pair and the theoretical model. The accuracy of the corner frequency strongly affects the stress drop estimation since stress drop has proportional relationship to the cube of the corner frequency. In this study, we introduce the residual evaluation to the corner frequency estimation process and select good quality of records toward the better stress drop estimation of potentially induced earthquakes in Oklahoma.

We chose  $M_w < 4.0$  events, and formed co-located ( $< 2$  km) event clusters using the events occurred from 2016 March 1st to August 31 ( $1.6 < M_L < 3.5$ ). The spectral ratios between the smaller events and the larger event in each cluster were calculated to remove path effects. Spectral ratios of the all components of 4 USGS and OGS stations which sampling frequency were 100 Hz were stacked. We analyzed 5.12 seconds from 2.5 times after the *S* wave arrival time after applied the band-pass filter of 0.1 to 40 Hz. Corner frequencies and moment ratio of each event pair were searched by the least square fitting with Brune model.

To improve the quality of the result, we evaluate the residual of the fitted curve to check the existence trade-off between two corner frequencies. We performed grid search between 1 to 30 Hz for a larger event and 1 to 60 Hz for a smaller event, and obtain the residuals (data minus model) on each data point at each trial. We displayed the residual map as a monochrome image, and calculate the distance between the smallest residual point and the centroid of the low residual region. We defined the event pairs which met the threshold distance of eight as a good quality data, and utilized them for the stress drop calculation. Comparing to the results without the selection, stress drops of selected data in the same cluster showed small variation in three clusters; thus, the quality control with residual would be effective. Estimated stress drops were 1-10 MPa for the smaller events and 6-63 MPa for the larger events. This result is consistent with the stress drop estimated in other regions of central United States as well as natural earthquakes.

Keywords: Stress drop, Corner frequency

# Precise Data Analyses toward the Update of Earthquake Source Spectral Model

\*Takahiko Uchide<sup>1</sup>, Kazutoshi Imanishi<sup>1</sup>

1. Geological Survey of Japan, National Institute of Advanced Industrial Science and Technology (AIST)

Earthquake source spectra are useful for simplifying, generalizing and differentiating properties of earthquakes rupture process. The standard model for source spectra is the  $\omega^2$ -model, in which the spectrum is flat at lower frequencies and decays as inversely proportional to the square of frequencies at high frequencies. The low and high frequency bands are bordered by the corner frequency, which is used for estimating stress drop under an assumption of a circular crack model.

One of the methods to improve the resolution of earthquake source spectra is the multiple spectral ratio analysis method [*Uchide and Imanishi*, BSSA, 2016], in which we employ multiple empirical Green's functions (EGF) to cancel the path and site effects as well as errors due to the differences in source locations and focal mechanisms of a target and EGF events. They applied this method to small earthquakes ( $M_w$  3.2 –4.0) in Fukushima Hamadori and northern Ibaraki prefecture areas and found that the source spectra are well approximated by the  $\omega^2$ -model with bumps for some earthquakes, whereas for some other earthquakes the  $\omega^2$ -model fits very well. Then number of questions arise. Is this universal or only in this area? What is the physical meaning of bumps? What is the simple and inclusive model for earthquake source spectra?

In this study, we examined small inland earthquakes in Japan by the same method. The study area includes following areas: Kumamoto, where many of small earthquakes are preceded by the 2016 Kumamoto earthquake ( $M_w$  7.0); Wakayama, where the seismicity is constantly active. The result indicated that the findings of *Uchide and Imanishi* [2016] are also the case in other areas.

The  $\omega^2$ -model with a bump around the corner frequency can be described as a double-corner-frequency model, while that with a bump at frequencies higher than the corner frequency can be that with a steeper slope at high frequencies. In the case of a double-corner-frequency model, the lower corner frequency will correspond to the source duration. Since the lower corner frequency will be generally smaller than the corner frequency in case of the single-corner-frequency model, such as the  $\omega^2$ -model, the double-corner-frequency model will give us a longer source duration and then lower stress drop.

Then what will the higher corner frequency represent? To answer this question, we need investigate the scaling relationship of two corner frequencies and the source process in detail, which are left as future work.

Keywords: Earthquake Source Spectra, Spectral Ratio Analysis

## Stress drops and uncertainty resolution of repeating earthquakes at Parkfield

\*Jiewen Zhang<sup>1</sup>, Xiaowei Chen<sup>1</sup>, Rachel E. Abercrombie<sup>2</sup>

1. Conocophillips School of Geology and Geophysics, University of Oklahoma, 2. Department of Earth and Environment, Boston University

Earthquake stress drop is an important parameter that is closely associated with ground motion predictions and earthquake source properties. Estimating stress drop from corner frequency is superficially easy but subject to significant uncertainty. In the Parkfield segment, Abercrombie [2014] analyzed three repeating clusters, and found that the sampling rate and source complexity significantly affect the reliability of source parameters. Specifically speaking, low sampling rate from the surface stations is insufficient to resolve corner frequencies for small earthquakes when the corner frequency is beyond the Nyquist frequency. In this study, we aim at resolving the uncertainty in source parameters systematically by comparing results from stacking methods that averaging over many event-station pairs, and results from individual pair analysis methods that look into details for each earthquake.

We begin with the double-difference catalog in Northern California, and an existed catalog with several clusters of repeating earthquakes. Then we search for suitable EGF events for each cluster. We are now studying two event groups, one from the proposed clusters with <20 repeating earthquakes, and the other selected ourselves manually which consists of 406 events with numerous distinct repeating clusters. For our own clusters, we set 0.99 as the cross-correlation threshold following a bandpass filter of 2~40 Hz for repeating pairs that will potentially be utilized for spectral analysis. Both event groups have wide magnitude range from 0 to 3, and we only include channels in different networks with high sampling rates (for borehole network sampling rate is 250 Hz and for surface network only 100 Hz channels). Low sampling rate channels are excluded so that it becomes feasible to apply a wider extension of bandpass filter. Then we will choose a cluster with a rational number of repeating events, apply both improved stacking analysis methods and individual pair analysis to the selected clusters, and systematically assess their consistency and difference. Updated results will be reported at the meeting.

Keywords: Stress drop, repeating earthquakes, uncertainty resolution, Sampling rates

# Frictional and Radiated Energy for the Shallow Fault of the 2011 Tohoku-oki Earthquake

\*James Mori<sup>1</sup>

1. Earthquake Hazards Division, Disaster Prevention Research Institute, Kyoto University

Recent results from the Japan Trench Fast Drilling Project (JFAST) estimated the level of dynamic friction on the shallow portion of the fault that had the very large slip during the 2011 Tohoku-oki earthquake. During this Integrated Ocean Drilling Program (IODP) expedition, borehole samples were obtained from the plate boundary fault zone at 820 meters below the sea floor. Also, temperature monitoring in the borehole across the fault zone measured the level of frictional heat generated at the time of the earthquakes. From both high-speed laboratory experiments on the fault zone material (Ujiie et al., 2013) and the temperature observations across the fault zone (Fulton et al., 2013), the shear stress during the earthquake rupture was estimated to be about 0.6 MPa. This shear stress corresponds to a coefficient of friction of about 0.08 to 0.1.

Comparing these results with estimates of the radiated energy, which are derived from teleseismic body waves, shows that the radiated energy is larger than the frictional heat for the shallow portion of the fault. However, for the deeper portions of the fault, the frictional heat is larger. The shallow and deep portions of the megathrust have different proportions for the energy balance and, thus, different styles of faulting.

Keywords: Tohoku earthquake, radiated energy, frictional heat, JFAST

# Moment Tensor Inversion of Earthquakes in Turkey and Surroundings by Using Site-Specific Velocity Models

\*Musavver Didem Cambaz<sup>1</sup>, Ahu Mutlu<sup>1</sup>

1. Bogazici University Kandilli Observatory and Earthquake Research Institute

Turkey and its surrounding regions are tectonically active and have high-seismicity rates. The seismicity in the region is observed by the national networks of the Kandilli Observatory and Earthquake Research Institute, KOERI, and the Disaster and Emergency Management Presidency Earthquake Department, AFAD. The quality and quantity of seismic stations improved significantly after the 17 August 1999 Mw 7.4 Izmit earthquake. In the meantime, a number of focal mechanism catalogs were produced, covering different time periods. In this study, we perform a systematic MT inversion of earthquakes within Turkey between 2008 and 2015, using the dense seismic networks of KOERI and AFAD. The use of combined networks and sitespecific velocity models for the computation of MT inversion results in high-quality solutions of focal mechanisms. This homogeneous focal mechanism catalog provides important new information on the seismotectonics in this region.

Keywords: Earthquake, Seismicity, Moment Tensor Inversion

## Current frontiers in spatio-temporal b-value analysis

\*Thessa Tormann<sup>1</sup>, Laura Gulia<sup>1</sup>, Nadine Staudenmaier<sup>1</sup>, Antonio Petrucci<sup>2</sup>, Bogdan Enescu<sup>3</sup>, Stefan Wiemer<sup>1</sup>

1. Swiss Seismological Service, ETH Zurich, Switzerland, 2. Dipartimento di Fisica e Astronomia, University of Bologna, Italy, 3. Department of Geophysics, Kyoto University, Japan

The frequency-size-distribution of earthquakes, characterized by the b-value in the Gutenberg-Richter law, has been documented for its variation in space and time. In many examples it could successfully be related to physical parameters such as stress concentration in asperities or high pore pressures in geothermal regimes. A generically observed depth gradient supports the laboratory-based hypothesis of b-values being inversely dependent on differential stress, which is equally reflected in significant variation between observed b-values for different faulting styles. Temporal variation is more difficult to detect robustly since it is easily biased by spatial activation heterogeneity. However, retrospectively detected b-value decreases before large events have been documented on scales ranging from few days to decades, while post-mainshock significant increases of b-values especially in the highest slip patches have been observed.

Here, we present an overview of some of the latest advances in studying patterns in the size distribution. In these examples from different regions of the world, including the subduction zones around Japan, we bridge various scales: from the smallest detected events to the giant megathrust earthquakes, from large-scale tectonic imprints to local heterogeneity along active faults, from temporally stable to time-varying patterns, from individual sequences to generic aftershock characteristics, from linear frequency magnitude distributions to those not following Gutenberg-Richter scaling, from low-b-focus to implications of observing very high b-values, from interpreting patterns in terms of physical processes to estimating future rupture potential.

Reliable b-value analysis is critically dependent on monitoring capabilities and homogeneous reporting of events. We demonstrate that improvements in this field are worthwhile: spatio-temporal b-value analysis has the potential to improve real time seismic hazard assessment and additionally provides many insights to advance the qualitative understanding of physical conditions and mechanisms.

Keywords: Gutenberg-Richter, b-value, spatio-temporal variation

## Along-fault velocity structure and its temporal changes on a laboratory granite fault undergoing stick-slip cycles.

\*Hiroki Sone<sup>1,2</sup>, Zirou Jin<sup>1</sup>, Lauren Abrahams<sup>1</sup>, Georg Dresen<sup>2</sup>

1. University of Wisconsin-Madison, 2. GFZ Potsdam

We conducted laboratory stick-slip experiments using a rough fault created in a granite sample, while passively monitoring acoustic emission (AE) events and actively monitoring the 2-D velocity structure along the fault plane. It has been observed in nature and lab that the b-value of earthquake frequency-magnitude relations have a negative correlation with stress magnitudes both spatially and temporally (Scholz, 1968; Schorlemmer and Wiemer, 2005), which may be useful for forecasting earthquake hazards from statistics of recorded earthquakes. However, the relation between the two parameters is empirical and is not supported by understanding of the underlying physics. While stress is not an easily observable parameter, velocity which may depend on stress can be observed through geophysical methods. We compare the spatial distribution of AE frequency-magnitude characteristics and the spatial distribution of ultrasonic wave velocity along the fault to seek for explanations to this empirical correlation. AE events and the velocity structure is monitored by 12 AE sensors wrapped around a rough fault created by breaking an intact granite cylinder (4 cm diameter) at 75 MPa confining pressure. The confining pressure is then raised to 150 MPa to promote stick-slip behavior during loading by a constant displacement rate, similar to Goebel et al. (2012). Periodic monitoring of the ultrasonic-wave travel time between the 66 AE sensor pairs indicate that travel times along each ray paths fluctuate systematically as the axial load cycles during multiple stick-slip events. We perform linear and non-linear inversion analyses using the observed travel times to reveal the change in velocity distribution along the fault plane. Preliminary results show that certain regions of the fault may be experiencing more velocity fluctuation than other regions of the fault. We will compare these fluctuations with the spatial distribution of AE events and its frequency magnitude characteristics to reveal any potential correlation that may help to explain the relation between b-values and stress.

Keywords: Acoustic Emission, P-wave tomography, Earthquake Parameters



# Remote triggering of earthquakes as a possible stress-meter: the case of the 2016 M7.3 Kumamoto mainshock

\*Bogdan Enescu<sup>1</sup>, Kengo Shimojo<sup>2</sup>, Anca Opris<sup>2</sup>, Yuji Yagi<sup>3</sup>

1. Department of Geophysics, Kyoto University, 2. Graduate School of Life and Environmental Sciences, University of Tsukuba, 3. Faculty of Life and Environmental Sciences, University of Tsukuba

## Introduction

Activation of seismicity at remote locations due to the passage of seismic waves from large earthquakes is a well-documented phenomenon (e.g., Hill et al. 1993). However, such distant earthquake triggering is scarce in Japan (e.g., Harrington and Brodsky, 2006) with the notable exception of the remote seismicity activated after the 2011 M9.0 Tohoku-oki earthquake (e.g., Miyazawa et al., 2011). Here we report on a relatively widespread remote triggering of small earthquakes following the 2016 M7.3 Kumamoto (Kyushu) earthquake (an inland, strike-slip event). We hypothesize that the observed, unusual remote triggering might relate with the crustal weakening at volcanoes after the 2011 Tohoku-oki earthquake. In addition, it may also relate with the tectonic stress levels of inland crustal faults.

## Data and Method

We have processed waveform data recorded at high-sensitivity Hi-net and broadband F-net stations, operated by NIED, as well as JMA and V-net (NIED) stations located throughout Japan. The waveforms have been scrutinized in both high and low frequency ranges to detect remote events that occurred during the passage of surface waves from the Kumamoto earthquake. Dynamic stresses have been estimated using the approach documented by Peng et al. (2009).

## Results and Discussion

The activated seismicity correlates well with the passage at the surface waves from the Kumamoto earthquake. The furthest triggered event was observed in Hokkaido, at ~1630 km epicentral distance, close to Akan volcano, one of the most active in Hokkaido. Another example of remote triggering is that at the Akita-Komagatake active volcano (epicentral distance of ~1191 km), in northern Honshu. Triggering has been also observed at other volcanoes in Tohoku, Chubu, close to Izu Peninsula, and in the southern part of Kyushu (at the Suwanose-jima volcano –the only remote triggering that occurred south of Kumamoto earthquake epicenter). While remote earthquake triggering at volcanoes is predominant, other regions of triggering include Wakayama, Tottori and Noto Peninsula, which correspond to active fault areas.

Since all the analyzed triggering cases take place at epicentral distances more than ~8 times the Kumamoto fault length (30 –40 km, Yagi et al., 2016), we infer that the static stress changes are too small to trigger seismicity at such distances. However, the dynamic stresses are significant, ranging from several kPa to tens of kPa. The threshold dynamic stresses that can trigger seismicity are of a few kPa (e.g., Aiken and Peng, 2014). Since most of the remotely triggered earthquakes have been observed at volcanoes, we suggest that the excitation of crustal fluids may have been the main triggering mechanism. The strong shaking, up to relatively large distances, due to a strong directivity effect, may explain the observed spatial distribution of the triggered earthquakes as well as their long-range extent.

It is critically important to understand why such widespread remote activation has not been observed before for Japan, at similar dynamic-stress levels. We have found out that the regions activated this time, in particular the volcanic areas in Tohoku, have been also activated (from days to weeks) after the 2011 Tohoku-oki earthquake. We hypothesize that mechanical weakening of a pressurized crust in these

regions due to the 2011 megathrust might be responsible for an increased trigger-ability. In addition, the activation of some active crustal faults might be related to the levels of tectonic stress along these fault lines. All these observations suggest that remote triggering might be used as a stress-meter at volcanoes and active faults.

**Reference paper:**

Enescu, B., Shimojo, K., Opris, A., and Y. Yagi, Remote triggering of seismicity at Japanese volcanoes following the 2016 M7.3 Kumamoto earthquake, *Earth, Planets and Space*, 68:165, doi:10.1186/s40623-016-0539-5, 2016.

Keywords: dynamic triggering, stress-meter, volcanoes, active faults, 2016 M7.3 Kumamoto earthquake

# Static stress triggering investigation for the 2016 Kumamoto sequence

\*Yuki Miyake<sup>1</sup>

1. Kyoto University, Disaster Prevention Research Institute

**[Overview]** I study the static triggering of the Kumamoto earthquake ( $M_{JMA}$  7.3) by two successive foreshocks. I especially examine which of the two foreshocks mainly contributed to the triggering of the mainshock by evaluating the static Coulomb stress change ( $\Delta CFS$ ). I also discuss which fault model fits better the seismicity.

**[Introduction]** There are two large foreshocks before the Kumamoto mainshock: the first one ( $M_{JMA}$  6.5) occurred 2.5 hours before the second one ( $M_{JMA}$  6.4). The much larger mainshock ( $M_{JMA}$  7.3) occurred 25.5 hours later. I have calculated the static stress change due to the two foreshocks on the fault-plane of the mainshock to examine the triggering characteristics of the sequence. As it is well-known,  $\Delta CFS$  shows whether slip on a fault (the “receiver”) is encouraged or inhibited due to slip on another fault (the “source”). It is usually difficult to reliably determine the  $\Delta CFS$  when the source and receiver faults are located nearby, since the stress estimation is sensitive to small variations of the fault-source slip distribution and its geometry. The hypocenters of the three events are within 10 km distance, so I assessed how much the estimated  $\Delta CFS$ s depend on it.

**[Comparison of fault models]** I need reliable fault models for the two sources and the receiver. There are several fault models available for the Kumamoto earthquakes; for example, the fault models obtained by inversion of InSAR data, the P-wave polarity FM solutions and the CMT solutions. I consider such solutions as “fault models” because one can approximate the fault width and height from the magnitude. I designed a software tool that enables to compare seismicity and faults in 3D. Using this tool, the user can easily plot any earthquake catalog - for example, the MFT catalog of the Kumamoto sequence (Kato et al. 2016) or the JMA catalog - as well as any fault/slip model. I found that the seismic activity from the first foreshock until the mainshock is distributed along several planes. I compared the plane-like distributions to the fault models and found the CMT solutions of the foreshocks to better fit the seismicity than the InSAR models. Thus, I decided to adopt these solutions as faults and changed incrementally their parameters to examine the effect on the  $\Delta CFS$ s.

**[Triggering characteristics]** The questions I try to answer are: (1) How much does the  $\Delta CFS$  depend on the source slip distributions? (2) Which of the two foreshocks more likely triggered the mainshock?

**[Method]** (1) I assumed that the slipping source fault is represented by its CMT solution and it shapes as a disc (circular fault); I calculated  $\Delta CFS$ s by changing incrementally the disc radius, as well as the dip and strike angles. The mechanism of the receiver fault (i.e., the mainshock fault) was that given by its FM solution. (2) I have done the same calculations for both source faults (i.e., for the two foreshocks).

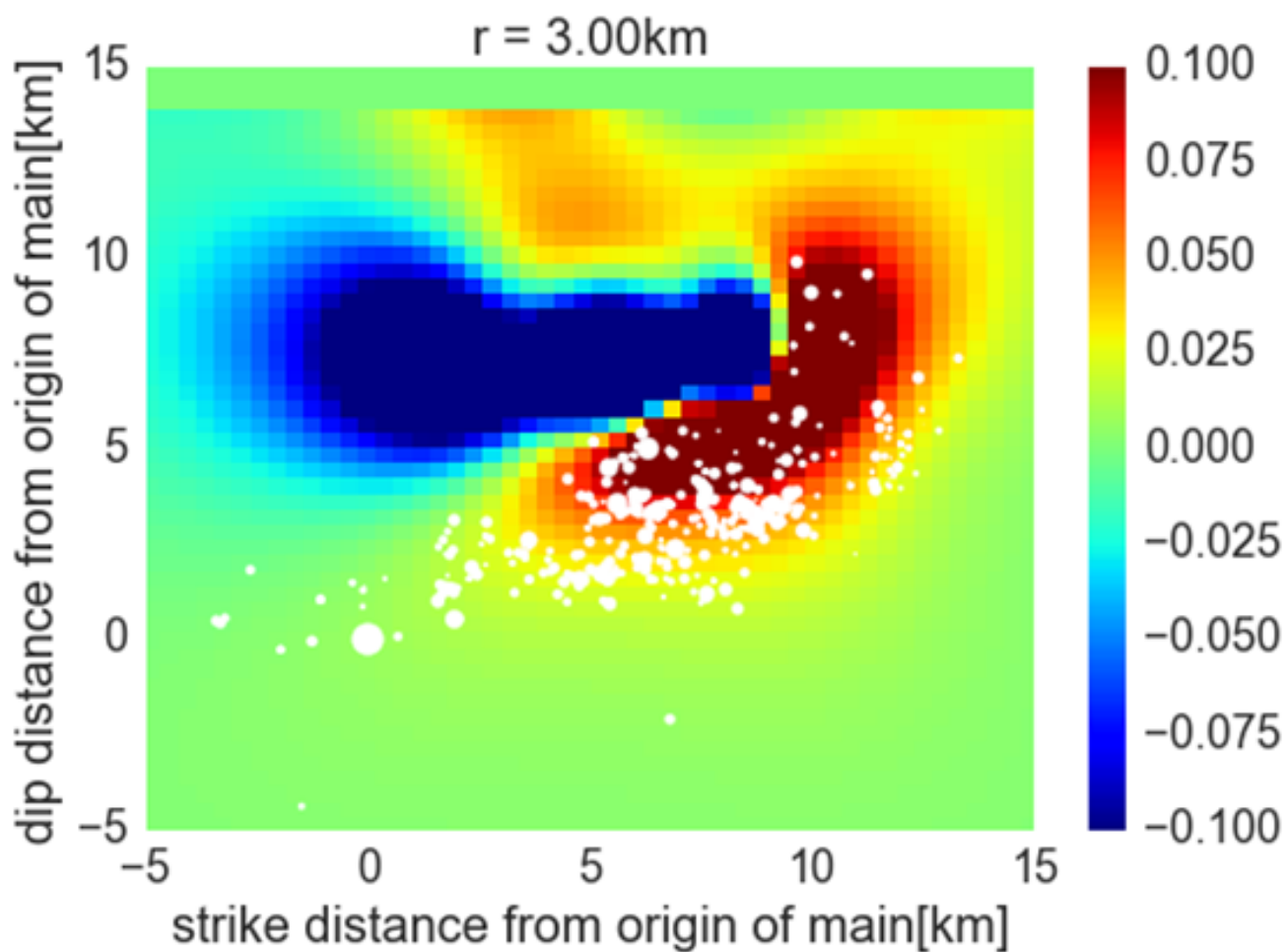
**[Results]** (1) The  $\Delta CFS$  depends less on the dip and radius of the slipping fault and more on its strike. This indicates that it is critically important to determine the strike angle accurately to evaluate the  $\Delta CFS$ . (2) The  $\Delta CFS$  due to the first foreshock was found to be more dependent on the radius of the disc (i.e., fault asperity). (3) The  $\Delta CFS$ s due to the first foreshock were larger than for the second foreshock, thus suggesting that the first foreshock likely triggered the mainshock. I have further considered the circular asperity of the first foreshock to overlap with the largest slip distribution on the foreshock fault plane, obtained by Asano et al. (2016). By computing the  $\Delta CFS$  for this asperity, I have obtained consistent large  $\Delta CFS$  values that support our results.

**[Conclusions]**

- (1) The first foreshock likely triggered the  $M_{JMA}$  7.3 Kumamoto mainshock, rather than the second one.
- (2) It is important to determine strikes of faults with accuracy to calculate  $\Delta CFS$ .

(3) The better fault parameters are those provided by the CMT solutions, rather than the InSAR fault model.

Keywords: seismicity, Kumamoto earthquake, fault model



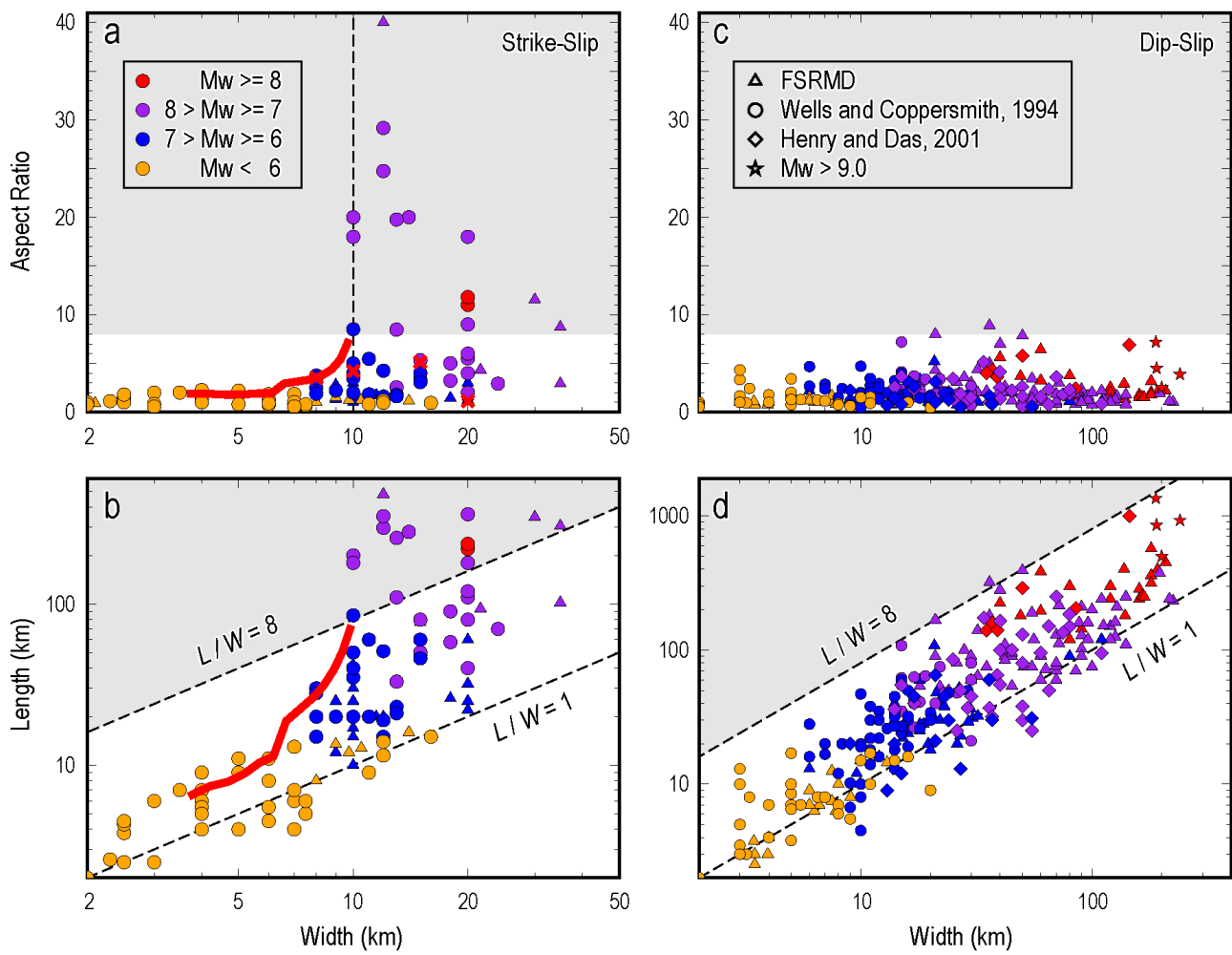
## Seismogenic width controls nucleation and aspect ratio of earthquake ruptures

\*Hongfeng Yang<sup>1</sup>, Huihui Weng<sup>1</sup>

1. Chinese University of Hong Kong

Whether the magnitude of earthquakes depends on the nucleation process is a key question in earthquake physics. Several observations of strike-slip and dip-slip earthquakes suggest that the eventual earthquake moment may increase with the size of the nucleation zone. However, it has also been proposed that the earthquake sizes may be not nucleation-related. We investigate the effect of seismogenic width on nucleation and aspect ratio of earthquake ruptures using numerical simulations of strike-slip faulting with a finite seismogenic depth (width). The seismogenic width has a significant effect on rupture propagation by controlling the energy balance near rupture tips. If the seismogenic width is smaller than a critical value, ruptures cannot propagate along the seismogenic fault continually, regardless of the size of the nucleation zone. The seismic moments of these self-arresting ruptures increase with the nucleation size, forming nucleation-related events. The aspect ratios increase with the seismogenic width but are generally smaller than 8, consistent with observations. In contrast, ruptures are breakaway ruptures and tend to have high aspect ratios ( $>8$ ) if the seismogenic width is sufficiently large. But the critical nucleation size for breakaway rupture is larger than the theoretical estimate for an unbounded fault. The eventual seismic moments of breakaway ruptures do not depend on the nucleation size. Our results suggest that estimating final earthquake magnitude from the nucleation phase may only be plausible on faults with small seismogenic widths.

Keywords: seismogenic width, rupture nucleation, rupture aspect ratio



## A Multiple Point Sources Study on the 2016 Kumamoto Mw 6.2 Earthquake

\*Shengji Wei<sup>1,2</sup>, Qibin Shi<sup>1,2</sup>, Meng Chen<sup>1,2</sup>

1. Earth Observatory of Singapore, Nanyang Technological University, 2. Asian School of the Environment, Nanyang Technological University

The Kumamoto  $M_w$  6.2 earthquake on April 14, 2016, which has been the first event in the 2016 Kumamoto earthquake sequence, occurring about one day before the  $M_w$  7.1 mainshock, shows significant complexity of its source. To understand the rupture history of the  $M_w$  6.2 earthquake, we employ a multiple-point-source inversion under the Markov Chain Monte Carlo (MCMC) scheme, where the earthquake rupture is decomposed into a set of point sources and each point source has respective focal mechanism, location, moment magnitude, rupture time and source duration. We use an  $M_w$  5.4 aftershock, which can be considered as point source, to calibrate the paths to all the strong motion stations within 100km. The calibration helps us to understand the sensitivity of the local velocity structure to the frequency we are using in the multiple point source inversion. The optimal model consists of three point sources with comparable moment magnitudes, indicating the moment of this earthquake was released three times from various part of the fault rupture. These three point sources are distributed around the intersection area of the Futagawa Fault and the Hinagu Fault, and the focal mechanisms are consistent with the fault geometry that is inferred from the relocated aftershocks, which dips to the southeast in the middle part and dips the northwest on the two side of the intersection area. The full moment tensor obtained by adding the contribution from each point source indicates a strong CLVD component, which is in agreement with the point source full moment tensor inversion result using the F-net and strong motion stations.

Keywords: Kumamoto Earthquake, Multiple point source, MCMC inversion

## Characteristics of subevents and rupture processes of the 2015 Mw 7.8 Gorkha Nepal earthquake from multiple-array back Projection

\*Weize Qin<sup>1</sup>, Huajian Yao<sup>1</sup>

### 1. USTC

On 25 April 2015 an Mw 7.8 earthquake occurred in Nepal and caused about 9000 casualties. This earthquake ruptured part of the Main Himalaya Thrust fault, which is due to the convergence of the subducting Indian plate to the overriding Eurasian plate, and showed thrust mechanism with a very small fault dip angle (about 7–10 deg). We apply teleseismic multiple-array back projection analysis to study the rupture process of this earthquake and find 6 clear high frequency radiation sources (subevents). Our results illustrate a simple unilateral eastward rupture of about 160 km with relative stable rupture speed of ~2.8 km/s and duration of 56 s. The entire rupture processes can be divided into 3 stages. The high frequency radiation appears to be mainly located at the edge of the large slip area, but the subevents have different characteristics in the western and eastern rupture areas. For this 2015 Nepal earthquake, the scales of asperities appear to be mainly controlled by depth, which dominates the overall patterns of slip and high frequency radiation. We finally propose a multiple-scale asperity model with stress and structural heterogeneities along the rupture direction to explain the distribution of high frequency subevents, co-seismic slip, and aftershocks. However, there exist some differences in the back projection results from different arrays. We attribute it to the 3-D structural heterogeneity in the source area. To solve this problem, referring to the former work of travel time calibration with aftershocks, we propose a new traveltimes calibration strategy using aftershocks with a spatial smoothing function in the inversion. This new method can produce results accounting for more reasonable velocity structures in the source area. We will further investigate the Gorkha earthquake rupture process with this new method to improve the multiple array back projection results.

Keywords: Nepal earthquake, Back projection, High frequency seismic radiation, Subevents, Rupture process



## Source rupture imaging using regional strong motion records

\*Tristan Deleplanque<sup>1</sup>, Jean-Pierre Vilotte<sup>1</sup>, Pascal Bernard<sup>1</sup>, Claudio Satriano<sup>1</sup>

1. Institut de Physique du Globe de Paris

The dynamic rupture of large earthquakes generates complex radiation with a large frequency range. The radiation complexity is induced by the fault geometry and the properties of the fault interface. For large earthquakes ( $M_w > 7.5$ ), teleseismic methods are used to study the rupture process at different frequency scales. For low frequency (LF) signals (50s -- 5s), inversion methods using kinematic models are well-established to determine the space-time distribution of the fault slip. On the contrary, for high frequency (HF) signals (1Hz -- 5Hz), even though models are more difficult to simulate, we can identify emission zones by the back projection method.

Large band spectral models of seismic sources are mainly kinematic. The slip distribution along the fault interface is modelled as a spatial and temporal stochastic process. At the fault scale, there is an effective rupture front propagation; and at small scale, we adjust the process to produce a spectrum which is consistent with the known seismic radiation. One of these models is the k-square model which superimposes a large number of asperities to produce one over k square final slip spectrum. The size of the asperities follows a power law distribution, they break with the rupture front passage and have a rising time proportional to their dimension.

Here, we want to improve the detail level of the HF images by using a regional network instead of a teleseismic one. The goal is to make our understanding of the rupture process better and to well-identify the link between HF radiation and the variability of strong ground motion. However, at regional scale, the heterogeneity of the crust implies a difference between the signals emitted along the fault from the point of view of one station; and the network aperture leads to a deformation of the phase shape of the Green function between stations. That is why there is not phase coherence anymore between two records. Therefore, by using characteristic functions (envelopes, kurtosis or Green functions), we want to extract the consistent information that lasts in the signal.

To do that, a known kinematic rupture, which is able to produce a correct HF radiation, is generated using a stochastic process. The different features of the rupture control the different frequency components of the source. We try to recover those features by back projection and have to deal with station distribution dependency or ghost signals.

### References:

C. Satriano, V. Dionicio, H. Miyake, N. Uchida, J.-P. Vilotte and P. Bernard (2015)  
Structural and thermal control of seismic activity and megathrust rupture dynamics in subduction zones: Lessons from the Mw 9.0, 2011 Tohoku earthquake  
Earth and Planetary Science Letters,  
doi: 10.1016/j.epsl.2014.06.037

J. A. Ruiz, D. Baumont, P. Bernard and C. Berge-Thierry (2011)  
Modelling directivity of strong ground motion with a fractal,  $k^{-2}$ , kinematic source model  
Geophysical Journal International,

doi: 10.1111/j.1365-246X.2011.05000.x

Keywords: large earthquake, earthquake rupture, regional network, imaging

## Microseismicity adjacent to the locked, late-interseismic Alpine Fault, New Zealand.

\*Calum John Chamberlain<sup>1</sup>, Carolin M Boese<sup>1</sup>, John Townend<sup>1</sup>

1. Victoria University of Wellington

New Zealand's Alpine Fault is the major on-land expression of the Australian-Pacific plate boundary, forming a dextral-reverse transpressional fault. The Alpine Fault is expected to fail in a great ( $M \sim 8.0$ ) earthquake in the coming decades, with a conditional probability of a large ground-rupturing earthquake in the next 50 years of 27%. The Deep Fault Drilling Project (DFDP) aims to study conditions on the Alpine Fault at depth prior to such a rupture. Motivated by the DFDP-2 drilling we conducted a focused study of microseismicity around the drill site, and subsequent real-time monitoring of seismicity during drilling. DFDP-2 was drilled in 2014-2015 in the Whataroa Valley, an area known to have low rates of seismicity, with few earthquakes above  $M_L 3.0$ .

To detect microseismicity in this seismically quiet region we used data from a dense local network of shallow borehole seismometers alongside data from the New Zealand national seismic network (GeoNet). We generated an initial catalog using standard energy-based detection techniques and manual phase-picks. From this initial catalog, 63 well recorded earthquakes within 20km of the DFDP-2 drill-site, and 14 explosions from a nearby quarry were selected for use as templates. These were used in a subsequent matched-filter detection routine through 2.25 years of continuous data. The resulting catalog contains 283 earthquakes of  $M_L < 1.8$  within 5km of the Alpine Fault surface trace. For all earthquakes, correlation pick-corrections were calculated to provide precise relative arrival times for use in double-difference hypocentre calculations. For highly similar earthquakes, precise magnitudes were calculated using the singular-value decomposition method. The resulting catalog of microseismicity is dominated by clustered, non-repeating seismicity in the vicinity of the main plane of the Alpine Fault, however the seismicity does not define a single fault structure. Based on evidence from this study and nearby geodetic studies, we infer that the Alpine Fault at the location studied is currently locked and accumulating stress throughout the seismogenic zone. Following this work we conducted real-time monitoring of seismicity around the DFDP-2 drill-site during drilling to study whether any changes in seismicity occurred during drilling. Little seismicity during drilling was detected around the borehole (4 earthquakes detected within 10km of the borehole), with no response observed due to drilling.

Keywords: Seismology, Deep-Fault Drilling Project, Alpine Fault

## Seismicity Rate as an Indicator of Stress Change: Case of the Northern Ibaraki Prefecture Area

\*Takahiko Uchide<sup>1</sup>

1. Geological Survey of Japan, National Institute of Advanced Industrial Science and Technology (AIST)

Seismicity rate is sensitive to the change in the stress applied on the fault.

I studied the northern Ibaraki prefecture area, where two large earthquakes in March, 2011 and a large normal faulting earthquake (Mj 6.3) on December 28, 2016 struck probably due to the coseismic and postseismic deformation of the 2011 Tohoku-oki earthquake [*Uchide et al.*, this meeting]. The GNSS data from GEONET of Geospatial Information Authority of Japan (GSI) infers a rapid extension in the east-west direction right after the Tohoku-oki earthquake and a slow east-west compression for a couple of years, which seems to contradict the generation of the large normal faulting event. The GNSS data is the measurement on the ground surface, and the strain rate at depth may be different. Therefore we examine the stress change using the seismicity rate based on the ETAS model [*Ogata*, 1988].

Using *etas\_solve* program [*Kasahara et al.*, 2016], the Japan Meteorological Agency (JMA) Unified Earthquake Catalog, I estimate the ETAS parameters for the 100-500 days from March 11, 2011 on which the Tohoku-oki earthquake occurred. I converted the JMA magnitude into the moment magnitude as proposed by *Uchide and Imanishi* [submitted]. A preliminary result suggested that the seismicity rate is more attenuating than the prediction by the ETAS model with the estimated parameters. This may indicate the attenuation in the shear stress on the fault.

Keywords: ETAS Model, Northern Ibaraki Prefecture Area